NATIONAL ADVISORY COMMITTEE FOR AERONAUTICS

TECHNICAL NOTE 3734

TURBULENT-HEAT-TRANSFER MEASUREMENTS AT A MACH NUMBER OF 3.90

By Maurice J. Brevoort

Langley Aeronautical Laboratory
Langley Field, Va.

Washington

July 1956

1Z

NATIONAL ADVISORY COMMITTEE FOR AERONAUTICS

TECHNICAL NOTE 3734

TURBULENT-HEAT-TRANSFER MEASUREMENTS AT A MACH NUMBER OF 3.90

By Maurice J. Brevoort

SUMMARY

Turbulent-heat-transfer measurements were obtained through the use of an axially symmetric annular nozzle which consists of an inner, shaped center body and an outer cylindrical sleeve. Measurements taken along the outer sleeve gave essentially flat-plate results that are free from wall interference and corner effects for a Mach number of 3.90 and for a Reynolds number range of 6.3×10^5 to 7.0×10^7. The heat-transfer-coefficient results are slightly higher than theoretical results for a Mach number of 4.0 and for a ratio of inside-surface temperature to free-stream temperature of 4.2. The temperature-recovery factors range from approximately 0.89 at a Reynolds number of 6.3×10^5 to approximately 0.86 at a Reynolds number of 7.0×10^7.

INTRODUCTION

The design of high-speed aircraft and missiles requires engineering information about heat-transfer coefficients and temperature-recovery factors for high speeds that extend over a wide range of Reynolds number. In references 1, 2, 3, and 4, local turbulent-heat-transfer measurements are presented for Mach numbers of 3.03, 2.06, 1.62, and 0.87, respectively.

The purpose of this investigation is to extend the work of references 1 to 4 to a Mach number of 3.90. The same type of apparatus and method of reducing the data was used in this investigation as employed in references 1 to 4. The range of Reynolds number for which measurements were obtained is from 6.3×10^5 to 7.0×10^7. The ratio of the inside-surface temperature to free-stream temperature varied from 4.2 to 3.5.

SYMBOLS

c	specific heat of sleeve material, Btu/(lb)($^{\circ}$R)
c_p	specific heat of air at constant pressure, Btu/(lb)($^{\circ}$R)
g	acceleration due to gravity, ft/sec^2
h	heat-transfer coefficient, Btu/(sec)(sq ft)($^{\circ}$R)
k	heat conductivity, Btu/(sec)(ft)($^{\circ}$R)
M	Mach number
Nu	Nusselt number, hx/k
Pr	Prandtl number, $\mu c_p g/k$
R	Reynolds number, $\rho V x/\mu$
St	Stanton number, $\frac{Nu}{R\ Pr} \equiv \frac{h}{\rho V c_p g}$
T_{av}	average wall temperature, $^{\circ}$R
T_e	effective stream air temperature at wall; some temperature which gives a thermal potential which is independent of heat-transfer coefficient, $^{\circ}$R
T_t	stagnation temperature, $^{\circ}$R
T_w	inside-surface temperature of nozzle sleeve, $^{\circ}$R
T_∞	free-stream temperature, $^{\circ}$R
t	time, sec
V	free-stream velocity, ft/sec
w	specific weight of sleeve material, lb/sq ft
x	longitudinal distance along sleeve, ft (unless indicated otherwise)

η_r recovery factor, $\frac{T_e - T_\infty}{T_t - T_\infty}$

μ dynamic viscosity coefficient, lb-sec/sq ft

ρ free-stream density of air, slugs/cu ft

APPARATUS AND METHOD

The apparatus consisted of an axially symmetric annular nozzle which was directly connected to the settling chamber of one of the cold-air blowdown jets of the Langley gas dynamics laboratory. The nozzle had a shaped wooden center body and two outer sleeves. One sleeve was constructed of 8-inch-diameter, extra heavy, seamless, carbon-steel pipe, and the other sleeve was constructed of 1/16-inch stainless steel which was rolled into a cylinder and welded. Both of the cylinders were surface machined inside and outside to wall thicknesses of 0.388 inch and 0.060 inch, respectively. The coordinates of the center body are given in table I. Another nozzle of similar construction, having a sleeve wall thickness of 0.750 inch, an inside diameter of 11.000 inches, and an overall length of 84 inches, was used for part of the tests.

A detailed drawing of the apparatus is shown in figure 1 which gives the locations of the thermocouples and static-pressure orifices. Details of the apparatus and measuring equipment are given in references 1 and 2. The Mach number distribution is shown in figure 2.

For this investigation, test runs were made for settling-chamber pressures of 31, 353, 395, and 410 lb/sq in. gage. Excluding the first 20 seconds, the pressures were maintained constant for each test run. The stagnation temperature started at essentially room temperature, decreased as the piping was cooled, and at an arbitrary time increased due to the addition of heat. This variation is illustrated in figure 3 where stagnation temperature is plotted against time for a settling-chamber pressure of 353 lb/sq in. gage.

The wall temperature started approximately at the stagnation temperature and tended to approach the equilibrium temperature which was approximately 50° R below stagnation temperature. This variation is shown in figure 4 where wall temperature at station 14 is plotted against time for a settling-chamber pressure of 353 lb/sq in. gage.

In figure 5 are plotted, for various times during the test run, the values of wall temperature against longitudinal distance along the cylinder. These values were used to determine the rate of change of the

longitudinal conduction $k\frac{d^2T_{av}}{dx^2}$ along the cylinder. Test results were taken only for the length of the cylinder for which $k\frac{d^2T_{av}}{dx^2} = 0$.

REDUCTION OF DATA

The equations used in reducing the data are

$$\eta_r = \frac{T_e - T_\infty}{T_t - T_\infty} \tag{1}$$

$$h = wc\frac{dT_{av}/dt}{T_w - T_e} \tag{2}$$

$$St = \frac{h}{\rho V c_p g} \tag{3}$$

and

$$Nu = St\ R\ Pr \tag{4}$$

The method consists of selecting a recovery factor and then obtaining T_e from equation (1). For each recovery factor that is selected, the corresponding quantity $T_w - T_e$ is determined and then plotted against the quantity $wc\frac{dT_{av}}{dt}$ (the heat input). The curve connecting these points is a straight line (eq. (2)). The true values of T_e and η_r are obtained when the line goes through zero. The slope of this line is the value of h. Figure 6 shows the values used in determining the recovery factor and h at station 14 for a settling-chamber pressure of 353 lb/sq in. gage.

The Stanton number is calculated from equation (3), and the Nusselt number is calculated from equation (4). The values of Prandtl number (0.71) and viscosity of air were taken from reference 5 and were based upon T_w. The value of T_w used was that value measured 80 seconds after starting. The values of specific heat and specific weight of the sleeve material were also taken from reference 5.

RESULTS AND DISCUSSION

Figure 7 shows the variation of local Nusselt number with local Reynolds number. The value of x used in evaluating these numbers has been adjusted for x = 0 location (the effective beginning of the turbulent boundary layer) by the method of references 1 and 2. The x = 0 locations are 4.0 inches downstream of the minimum station for a settling-chamber pressure of 31 lb/sq in. gage and 10.0 inches upstream of the minimum station for the other pressures. The Nusselt numbers were found to vary from 400 to 23,000 for the Reynolds number range of 6.3×10^5 to 7.0×10^7. For comparison, the curves for $M = 4.0$ and $T_w/T_\infty = 4.2$ of the Van Driest analysis (ref. 6) are shown. The average value of T_w/T_∞ for the test results was 4.2 to 3.5. The data were computed by using free-stream temperature to determine the density and velocity. The wall temperature was used to determine the viscosity and Prandtl number. The data are slightly above the $M = 4.0$ curve.

Figure 8 shows the variation of local temperature-recovery factor with local Reynolds number. The variation is from approximately 0.89 at 6.3×10^5 to approximately 0.86 at 7.0×10^7. Also included for comparison are the curves for the recovery factor equal to $Pr^{1/3}$ and $Pr^{1/2}$. The wall temperature was used to determine the Prandtl number.

CONCLUDING REMARKS

Turbulent-heat-transfer measurements that gave essentially flat-plate results were obtained for a Mach number of 3.90 and for a Reynolds number range of 6.3×10^5 to 7.0×10^7. The Nusselt numbers are slightly higher than the theoretically derived Nusselt numbers for a Mach number of 4.0. The temperature-recovery factors show a decrease with Reynolds number from approximately 0.89 at 6.3×10^5 to approximately 0.86 at 7.0×10^7.

Langley Aeronautical Laboratory,
National Advisory Committee for Aeronautics,
Langley Field, Va., April 25, 1956.

REFERENCES

1. Brevoort, Maurice J., and Rashis, Bernard: Turbulent-Heat-Transfer Measurements at a Mach Number of 3.03. NACA TN 3303, 1954.

2. Brevoort, Maurice J., and Rashis, Bernard: Turbulent-Heat-Transfer Measurements at a Mach Number of 2.06. NACA TN 3374, 1955.

3. Brevoort, Maurice J., and Rashis, Bernard: Turbulent-Heat-Transfer Measurements at a Mach Number of 1.62. NACA TN 3461, 1955.

4. Brevoort, Maurice J., and Rashis, Bernard: Turbulent-Heat-Transfer Measurements at a Mach Number of 0.87. NACA TN 3599, 1955.

5. Eckert, E. R. G. (With Appendix by Robert M. Drake, Jr.): Introduction to the Transfer of Heat and Mass. First ed., McGraw-Hill Book Co., Inc., 1950, pp. 266 and 274.

6. Van Driest, E. R.: The Turbulent Boundary Layer for Compressible Fluids on a Flat Plate With Heat Transfer. Rep. No. AL-997, North American Aviation, Inc., Jan. 27, 1950.

TABLE I.- CENTER-BODY COORDINATES

x, in.	Radius, in.	x, in.	Radius, in.
-4.7	2.000	3.50	3.0295
-4.5	2.020	3.75	2.9555
-4.0	2.120	4.00	2.8834
-3.0	2.540	4.50	2.7473
-2.5	2.805	5.00	2.6221
-2.0	3.095	5.50	2.5067
-1.5	3.360	6.00	2.4002
-1.0	3.568	7.00	2.2093
-.8	3.635	8.00	2.0440
-.6	3.690	9.00	1.8995
-.4	3.732	10.00	1.7734
-.2	3.760	11.00	1.6647
0	3.7707	12.00	1.5722
.25	3.7640	13.00	1.4950
.50	3.7430	14.00	1.4324
.75	3.7116	15.00	1.3838
1.00	3.6739	16.00	1.3486
1.25	3.6289	17.00	1.3258
1.50	3.5774	18.00	1.3139
1.75	3.5203	18.782	1.3112
2.00	3.4585	19.00	1.3029
2.25	3.3927	20.00	1.2919
2.50	3.3237	25.00	1.2369
2.75	3.2520	30.00	1.1819
3.00	3.1786	35.00	1.1269
3.25	3.1042	37.50	1.0994
		40.50	1.9070

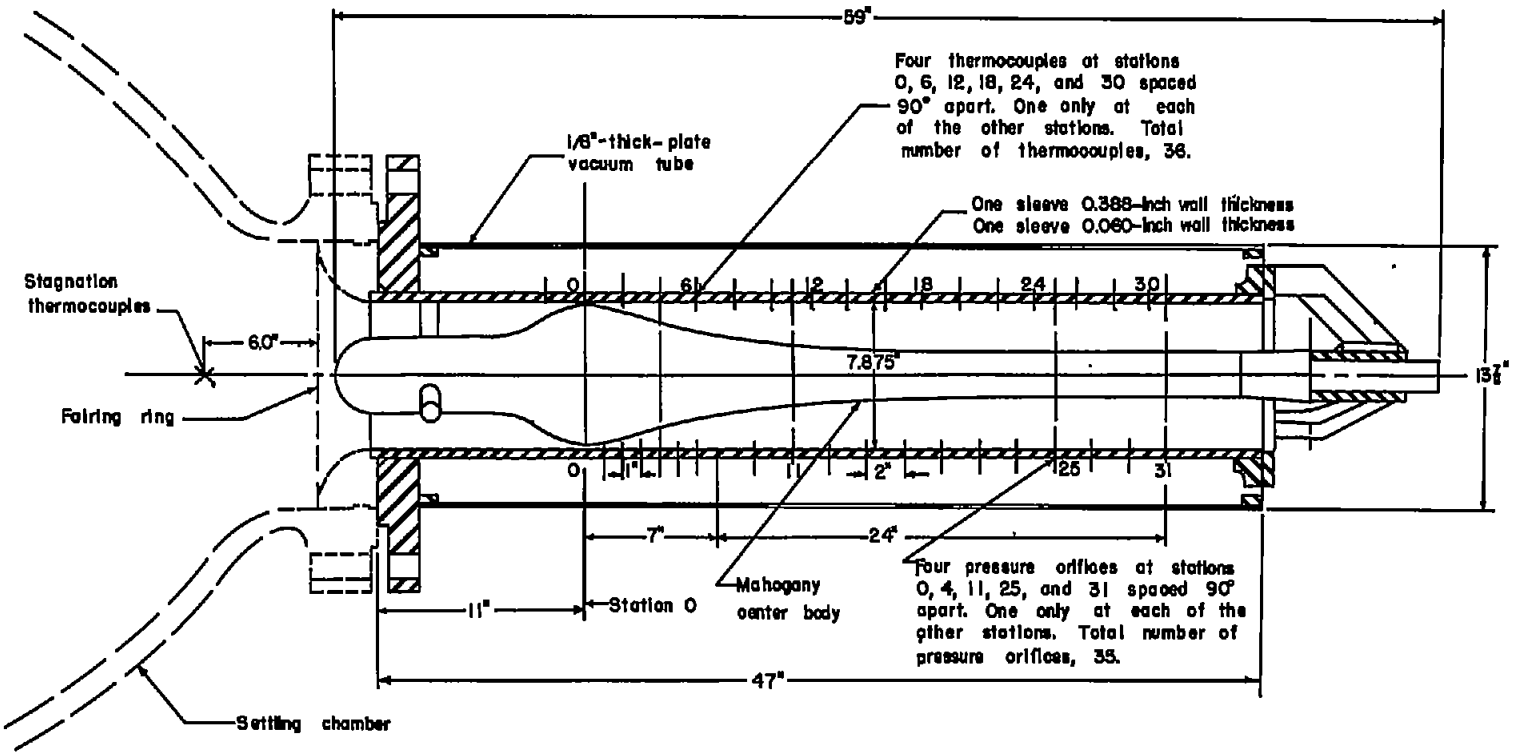

Figure 1.- Test setup.

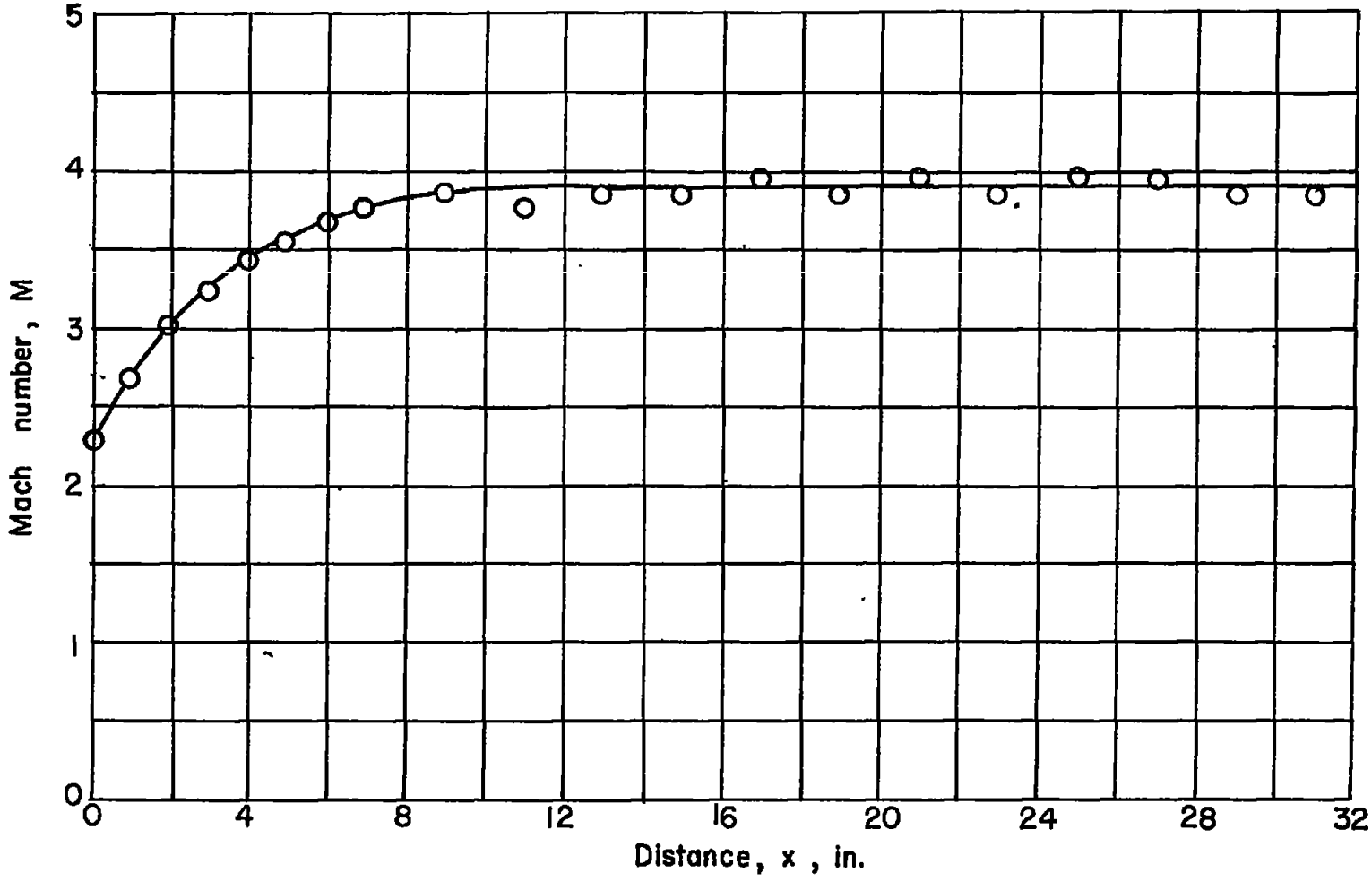

Figure 2.- Mach number distribution for settling-chamber pressure of 353 lb/sq in. gage.

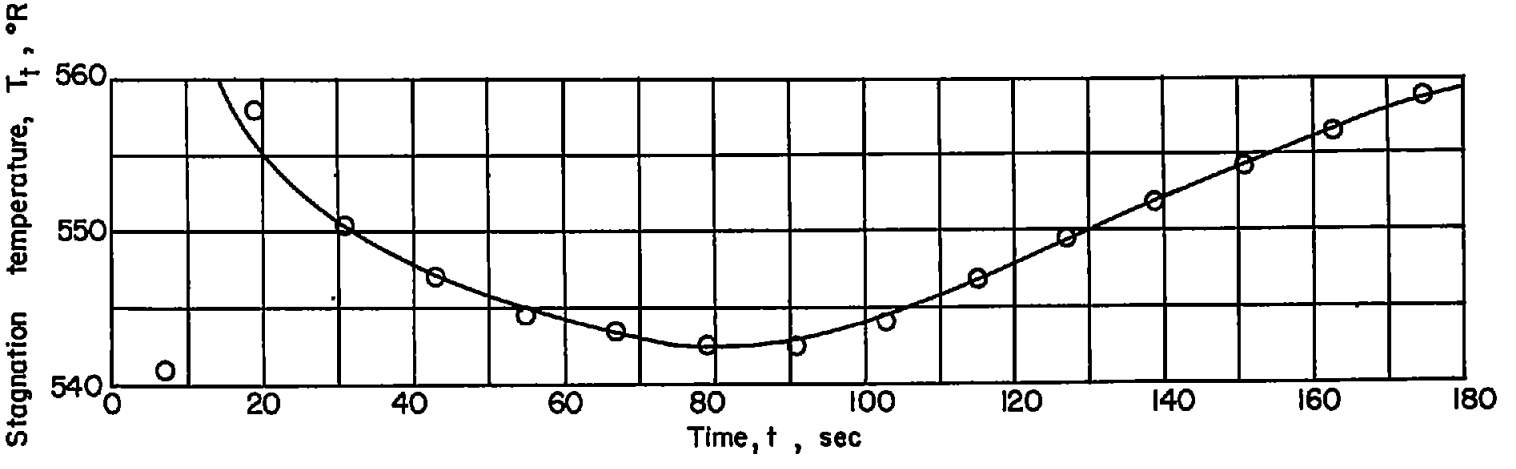

Figure 3.- Variation of stagnation temperature with time for a settling-chamber pressure of 353 lb/sq in. gage.

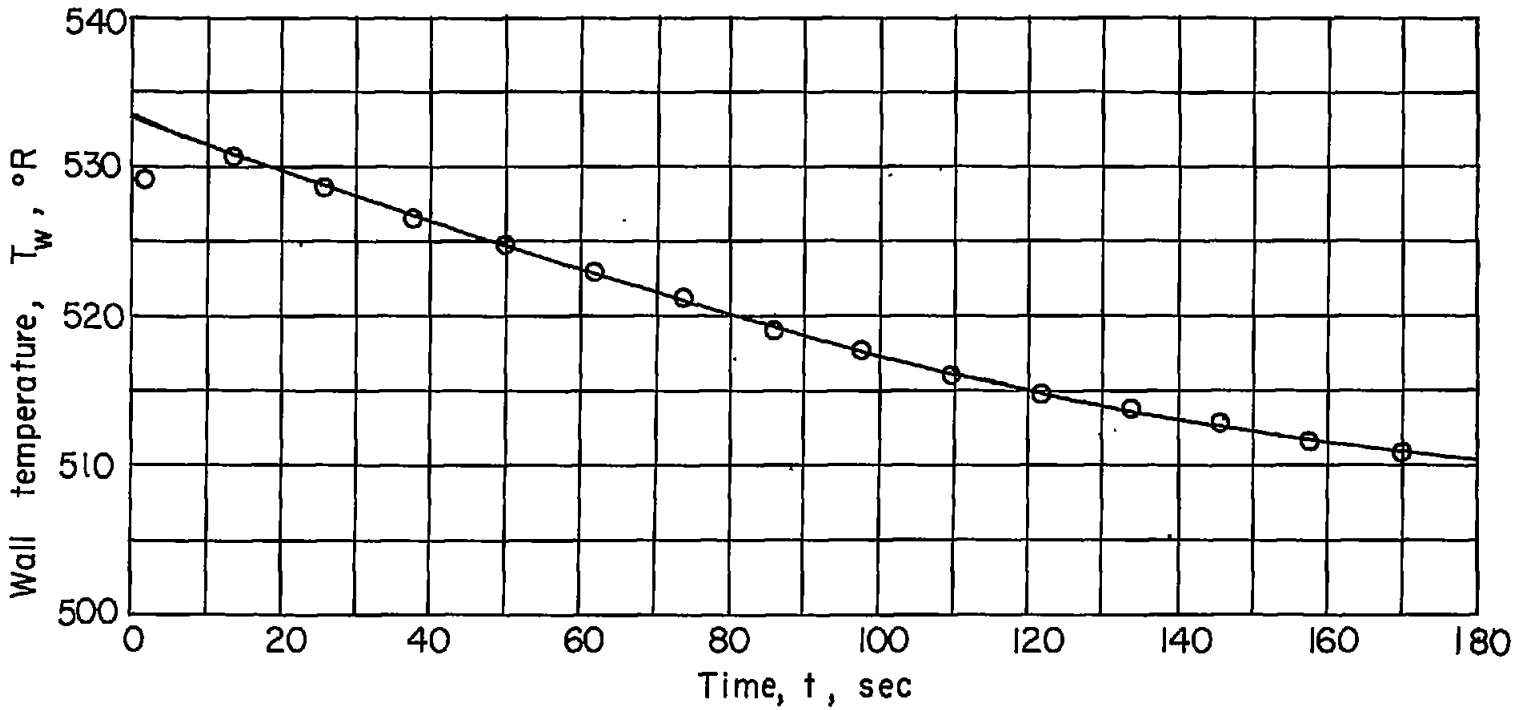

Figure 4.- Variation of wall temperature with time at station 14 for a settling-chamber pressure of 353 lb/sq in. gage.

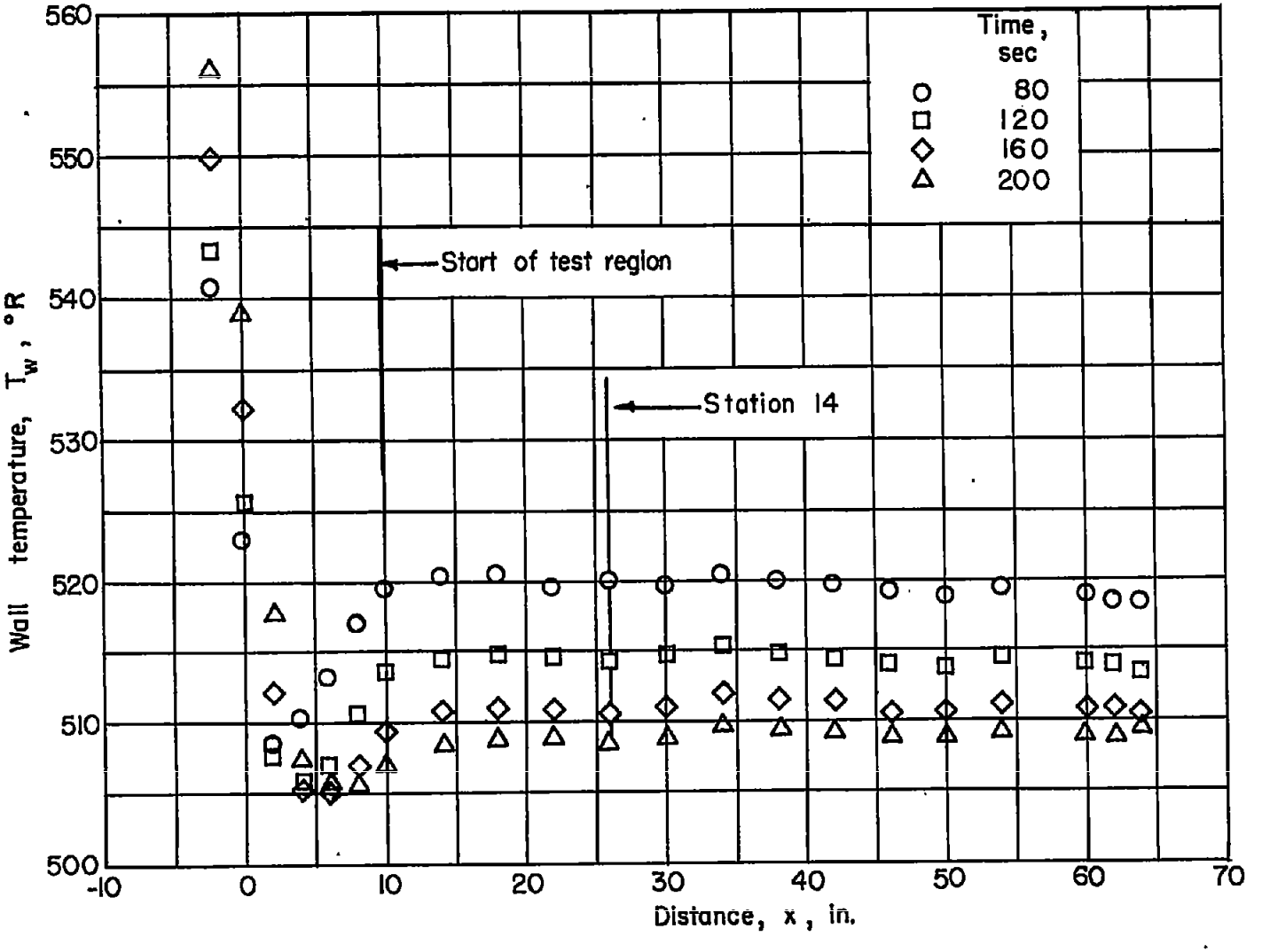

Figure 5.- Variation of wall temperature with longitudinal distance for a settling-chamber pressure of 353 lb/sq in. gage.

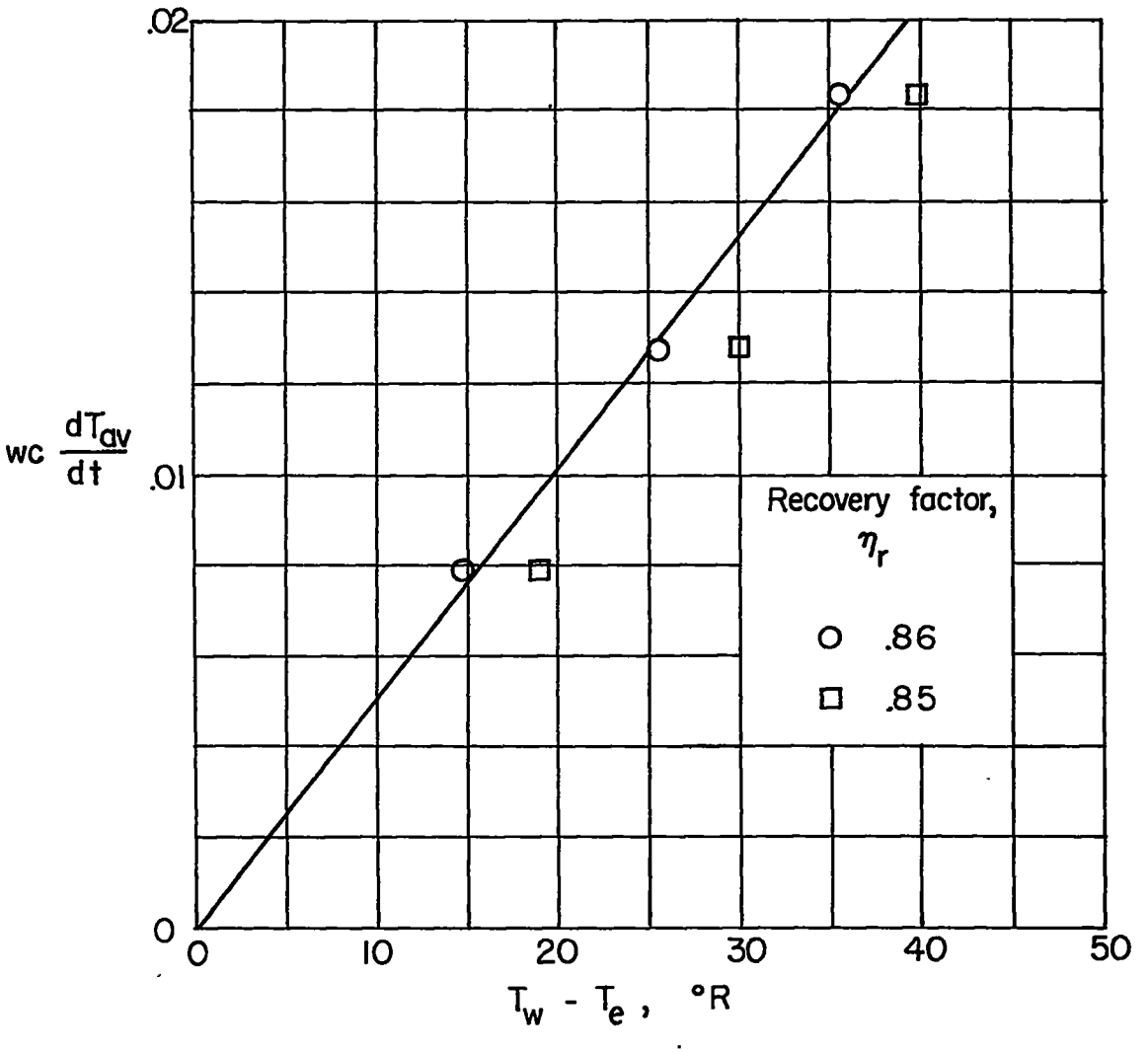

Figure 6.- Heat input as a function of recovery factor and $T_w - T_e$ at station 14 for a settling-chamber pressure of 353 lb/sq in. gage.

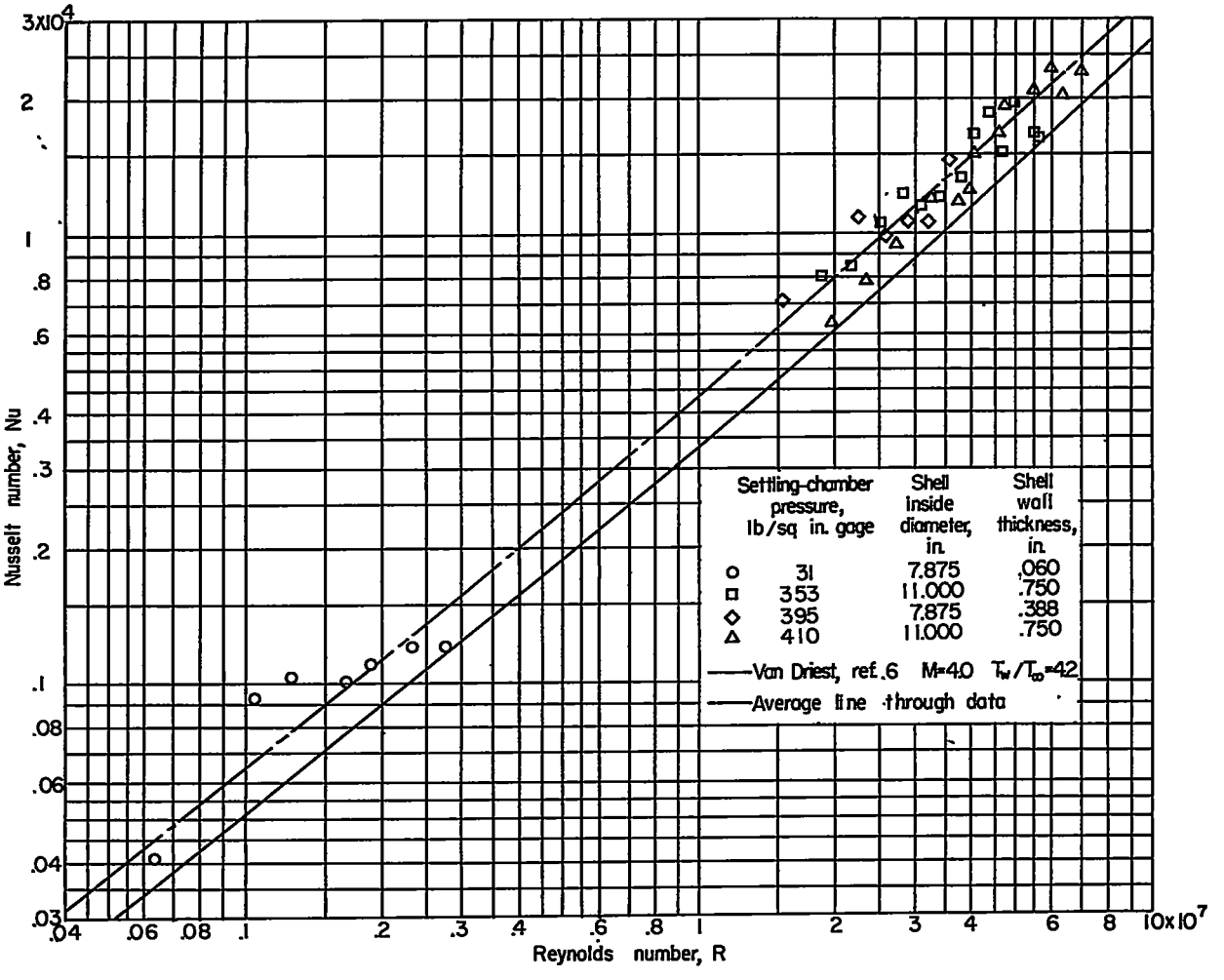

Figure 7.- Variation of local Nusselt number with local Reynolds number for corrected location of x = 0. Viscosity and Prandtl number determined for wall temperature.

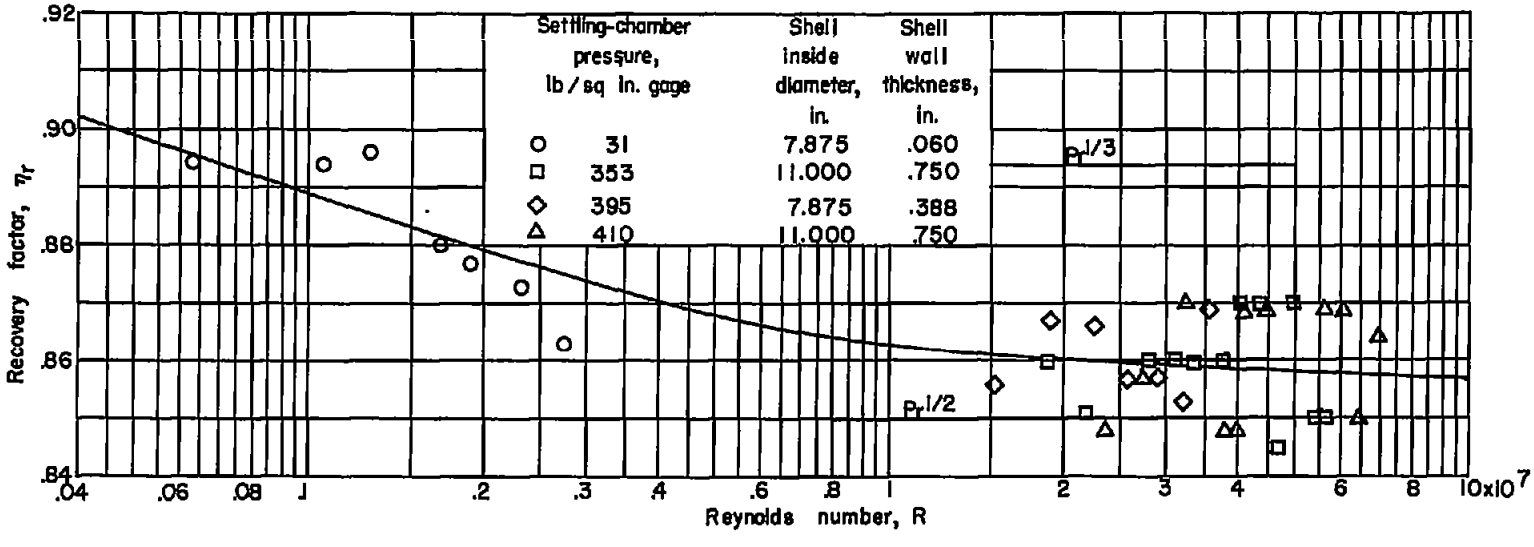

Figure 8.- Variation of local recovery factor with local Reynolds number for corrected location of x = 0. Viscosity determined for wall temperature.